# Evaluation of peri-implant bone defects on cone-beam computed tomography and the diagnostic accuracy of detecting these defects on panoramic images

Takayuki Oshima [ID][1], Rieko Asaumi [ID][1,*], Shin Ogura [ID][2], Taisuke Kawai [ID][1]

[1]*Department of Oral and Maxillofacial Radiology, The Nippon Dental University School of Life Dentistry, Tokyo, Japan*
[2]*Division of Oral Implantology, The Nippon Dental University Hospital, Tokyo, Japan*

## ABSTRACT

**Purpose**: This study was conducted to identify the typical sites and patterns of peri-implant bone defects on cone-beam computed tomography (CBCT) images, as well as to evaluate the detectability of the identified bone defects on panoramic images.

**Materials and Methods**: The study population included 114 patients with a total of 367 implant fixtures. CBCT images were used to assess the presence or absence of bone defects around each implant fixture at the mesial, distal, buccal, and lingual sites. Based on the number of defect sites, the presentations of the peri-implant bone defects were categorized into 3 patterns: 1 site, 2 or 3 sites, and circumferential bone defects. Two observers independently evaluated the presence or absence of bone defects on panoramic images. The bone defect detection rate on these images was evaluated using receiver operating characteristic analysis.

**Results**: Of the 367 implants studied, 167 (45.5%) had at least 1 site with a confirmed bone defect. The most common type of defect was circumferential, affecting 107 of the 167 implants (64.1%). Implants were most frequently placed in the mandibular molar region. The prevalence of bone defects was greatest in the maxillary premolar and mandibular molar regions. The highest kappa value was associated with the mandibular premolar region.

**Conclusion**: The typical bone defect pattern observed was a circumferential defect surrounding the implant. The detection rate was generally higher in the molar region than in the anterior region. However, the capacity to detect partial bone defects using panoramic imaging was determined to be poor. *(Imaging Sci Dent 2024; 54: 171-80)*

**KEY WORDS**: Radiography, Panoramic; Cone-Beam Computed Tomography; Peri-Implantitis; Bone Resorption

## Introduction

Regular maintenance of dental implants typically includes periodontal examination to assess plaque, probing depth, gingivitis, and the presence of bleeding and drainage, as well as X-ray imaging to evaluate bone defects. Additionally, the examination should assess implant mobility and the occlusal condition. If a bacterial infection leads to peri-implant mucositis, which then progresses to peri-implantitis, changes in bone morphology and quality can occur due to peri-implant alveolar bone resorption. This process resembles chronic periodontitis in the natural dentition.[1,2] When peri-implantitis is clinically suspected, the status of the surrounding bone should be evaluated using X-ray imaging.[3] Some guidelines recommend intraoral periapical radiography (using the paralleling technique) as the first choice for evaluating bone defects during maintenance. This technique minimizes radiation exposure and produces images with little distortion.[4-6] However, the paralleling technique can be challenging to use because the receptor must be positioned parallel to the implant fixture, the direction and angle of which are not visually confirmable. Moreover, the resulting image is 2-dimensional and offers a view from only a single direction, with the surrounding structures superimposed. Consequently, it is impossible to visualize the condition of the buccal/lingual bone near the implant fixture, which exhibits high X-ray attenuation.[7]

Recent years have brought a proliferation of implant manufacturers and types,[8] making it challenging to differentiate between the various implants that may have been placed. In addition, the increased use of angled abutments has contributed to variability in the orientation of implant placement, potentially complicating the understanding of the implant direction and angle. Although receptor-holding instruments are sometimes employed to perform the paralleling technique, this approach can be uncomfortable for patients with a shallow palatal vault or a low-lying floor of the mouth.[9] Additionally, the presence of multiple implant fixtures in many patients complicates the process of capturing images of each implant. Consequently, assessing bone defects on intraoral radiographic images can be a taxing process for both the operator and the patient.

In advanced peri-implant bone loss, deep V-shaped defects[10] and buccal dehiscence[11] around the implant are key factors that influence the choice of treatment – such as resection or regeneration – and the treatment outcome.[10-12] Therefore, objectively evaluating the morphology of the bone defect is crucial. Clinically, bone defects resulting from peri-implantitis vary, but they can generally be classified into suprabony and intrabony defect configurations.[13] Intraosseous defects are further categorized as bone defects in which the implant fixture is exposed through the bone surface due to dehiscence, defects of the bone wall on multiple lateral surfaces of the implant, or a combination of these types.[14] Consequently, it is necessary to perform not only mesiodistal observation but also 3-dimensional interpretation, including the buccal and lingual aspects. Three-dimensional imaging with dental cone-beam computed tomography (CBCT) is reportedly highly accurate in identifying alveolar bone defects and is clinically used to measure and classify peri-implant defects.[15] However, the radiation dose associated with CBCT is higher than that of intraoral radiography, and metal artifacts caused by the implant and surrounding structures can make it difficult to observe the interface between the implant and alveolar bone.[16,17] Therefore, guidelines do not recommend the routine use of CBCT for monitoring treatment results or disease progression[18] and state that CBCT should be reserved for use only in emergency situations.[19]

Kim et al.[20] suggested that conventional intraoral or panoramic radiography should be the preferred initial method for evaluating and monitoring the bone surrounding implant fixtures after achieving osseointegration. In clinical practice, panoramic radiography is used for maintenance and follow-up radiographic examinations due to its lower radiation dose compared to CBCT, the relatively small number of images required, and the simplicity of the panoramic radiographic procedures relative to intraoral radiography.[21-23] Panoramic radiography enables comprehensive screening of the hard tissue within and around the oral cavity. Its advantages over intraoral radiography include shorter imaging time and a simpler, less stressful examination for the patient.[24] Although both panoramic and intraoral images can be used to assess the mesiodistal bone status of an implant fixture at the alveolar crest level, the superposition of structures can hinder the identification of bone defects confined to the buccolingual aspect of the implant fixture. In such cases, the bone condition may need to be inferred from other clinical examinations, complicating the selection of diagnostic tests and the subsequent diagnosis. The objectives of this study were to identify the typical locations and patterns of peri-implant bone defects on CBCT images and to ascertain the factors influencing the detection of peri-implant bone defects on follow-up panoramic images.

## Materials and Methods

This study was conducted in full accordance with the 2013 Declaration of Helsinki (World Medical Association). The study protocol was approved by the relevant institutional review board (NDU-T2022-21). As this was a retrospective study, it was not possible to obtain informed consent from all patients. However, the purposes and methods of the study were made public, and patients were given the opportunity to opt out of participation.

### Study sample

This retrospective study incorporated images of 114 patients and 367 implant fixtures during the maintenance period, with these images acquired between 2018 and 2022.

The images were selected for inclusion if a minimum of 36 months had elapsed since the application of the superstructure and if both panoramic and CBCT images (with the latter taken for any reason) were obtained within a 1-month period.

Panoramic images were acquired using the Veraview X800 device (J Morita MFG Corp, Kyoto, Japan), with a tube current of 10 mA and a tube voltage of 69 kV. CBCT images were obtained with the FineCube system (Yoshida Dental Trade Distribution Co., Tokyo, Japan), utilizing a tube current of 4 mA and a tube voltage of 90 kV.

Images were excluded if the patient had a history of previous implant treatment in the same region, or if prior sur-
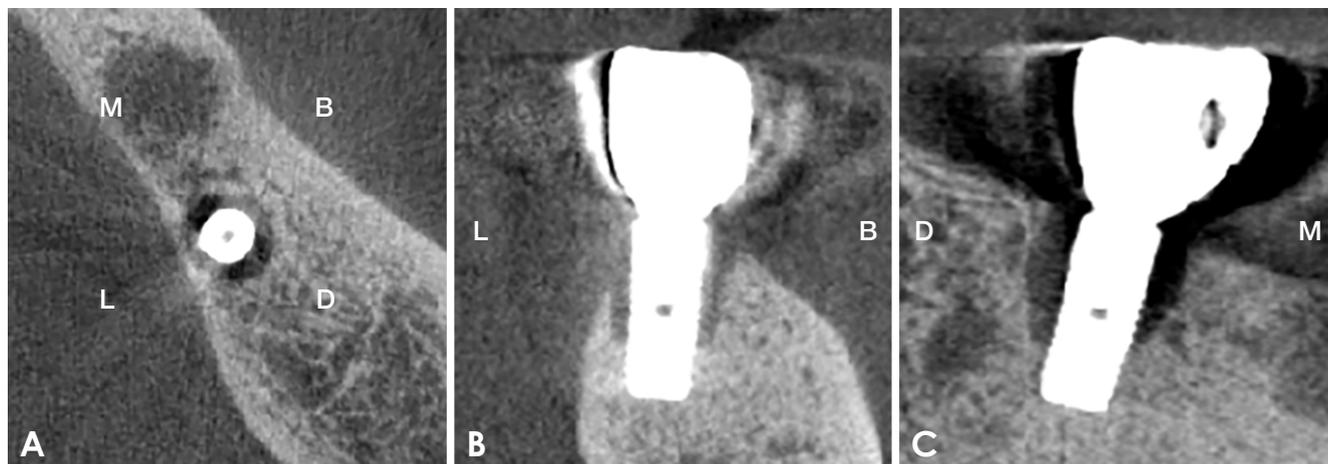
**Fig. 1.** Representative cone-beam computed tomographic images used to evaluate the presence or absence of bone defects at the mesial (M), distal (D), buccal (B), and lingual (L) sites around the implant. A. Axial image. B. Coronal image. C. Sagittal image.

gical intervention had been conducted due to bone fracture, inflammation, or cyst/tumor removal. The exclusion criteria also included disease in other parts of the maxillofacial region that could affect the jawbone area; insufficient image quality for interpretation due to poor positioning, movement, or severe metal artifact; and any other reasons that led observers to judge the images as overly difficult to interpret.

Two oral radiologists independently assessed the placement area of each implant fixture on CBCT. This evaluation was aimed at ascertaining the presence or absence of bone defects, including the sites and patterns of defects around all implant fixtures. The implant placement regions were categorized into 6 areas: anterior teeth, premolars, and molars in both the maxilla and mandible. Bone defect patterns were classified according to the site of the defect as revealed by CBCT. Figure 1 presents representative CBCT images used to determine the presence or absence of bone defects at the mesial (M), distal (D), buccal (B), and lingual (L) sites around the implant. In cases of disagreement between the 2 observers, a consensus was reached through discussion. Additionally, the overall pattern of bone defects was categorized into 3 types based on the number of bone defect surfaces in contact with the implant fixture. This modified classification, based on a report by Monje et al.,[7] is depicted in Figure 2. The patterns were defined as follows: a single site with a bone defect (M, D, B, or L), 2 or 3 sites with bone defects (2 sites: MD, BL, M + B or L, D + B or L; 3 sites: MD + B or L, BL + M or D), or 4 sites with bone defects, the last of which constitutes a circumferential defect (MDBL).

The reliability of the results was evaluated by analyzing the assessments of 2 observers with expertise in oral implantology. Observer 1 had 25 years of experience, while observer 2 had 10 years. They were tasked with determining the presence or absence of bone defects on the M, D, B, and L aspects of the implant fixture. For buccolingual defects, the observers were instructed to categorize the defects simply as "buccal or lingual." Each observer independently reviewed the panoramic images on 2 separate occasions, with the first review occurring at least 2 weeks prior to the second. The observations were conducted under the following conditions: 1) all images were viewed on the same Radiforce MX216 monitor (EIZO Corp, Ishikawa, Japan; resolution: 1600 × 1200) using Viewer 9.0 (export version; PSP Corp, Tokyo, Japan); 2) the observations were made at a consistent time of day; 3) observers were permitted to adjust the contrast and magnification of the images; and 4) a random number table, generated with Microsoft Excel 2019 (Microsoft Corp, Redmond, WA, USA), was used to randomize the order in which the images were presented for observation.

Figure 3 displays a representative panoramic image used to assess bone defects around an implant. The detection rate was determined by averaging the values from the 2 observers identifying bone defect sites (M, D, B, or L) on panoramic images, with the CBCT findings serving as the reference standard.

### Statistical analysis

All observation results were summarized using Microsoft Excel 2019. Regarding the detection rate of bone defects on panoramic images, receiver operating characteristic analysis was performed to calculate the area under the curve (AUC). Additionally, Cohen weighted kappa values were computed to quantify the inter-observer agreement on the evaluation
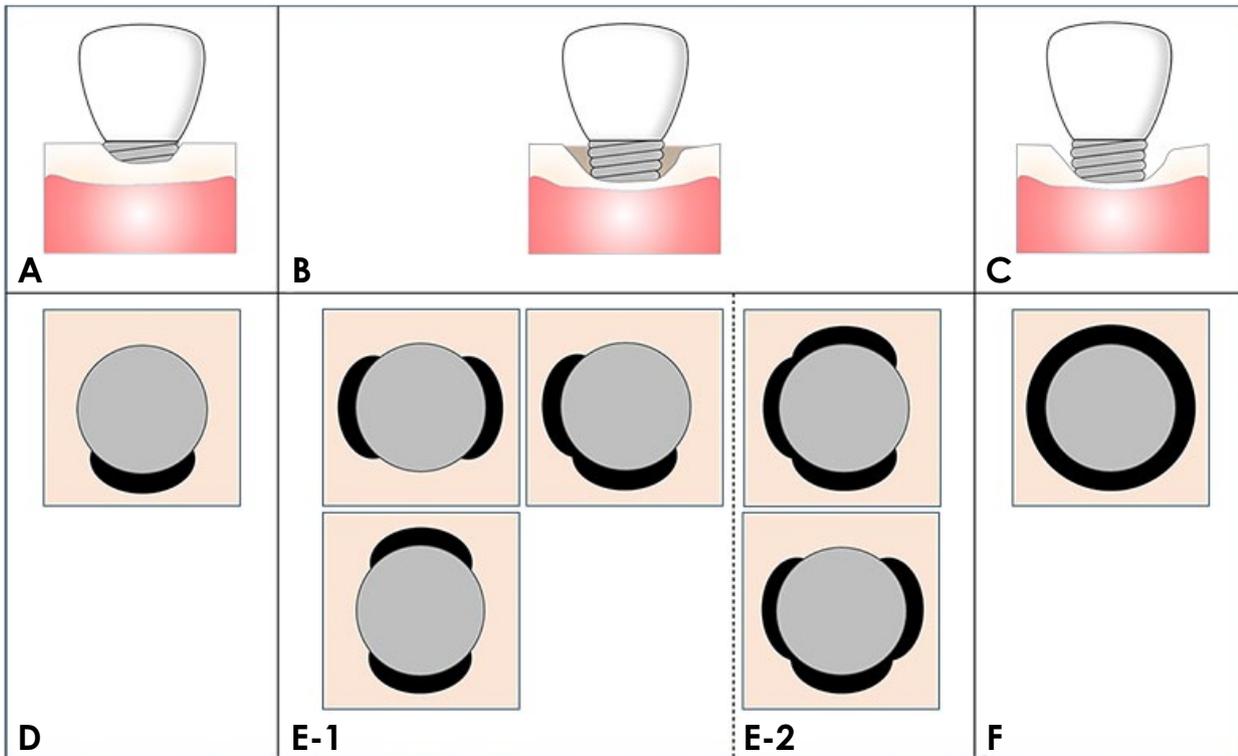
**Fig. 2.** Schematic illustration of the bone defect morphologies. Defects were classified into 3 patterns based on the number of bone surfaces in contact with the implant fixture observed. A-C. Buccal (lingual) view. D-F. Occlusal view. A and D. A single site with a bone defect (M, D, B, or L). B and E. Two or 3 sites with bone defects. E-1. Two sites with bone defects (MD, BL, M＋B or L, D＋B or L). E-2. Three sites with bone defects (MD＋B or L, BL＋M or D). C and F. Four sites with bone defects (MDBL, i.e. a circumferential defect). M: mesial, D: distal, B: buccal, L: lingual.
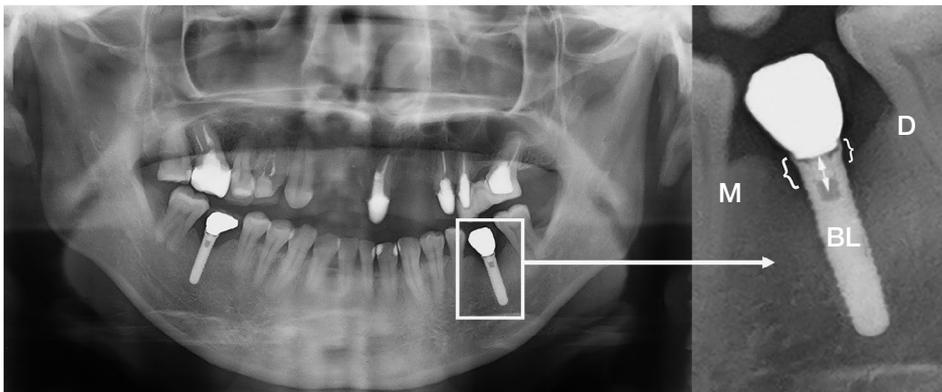


**Fig. 3.** Representative panoramic images used to assess the presence or absence of bone defects at the mesial (M), distal (D), buccal (B), and/or lingual (L) sites around the implant.

of bone defects. All statistical analyses were performed using SPSS (version 27.0, IBM Corp., Armonk, NY, USA). The kappa values were interpreted as follows: values less than 0.00 indicated poor agreement, 0.00-0.20 indicated slight agreement, 0.21-0.40 indicated some agreement, 0.41-0.60 indicated moderate agreement, 0.61-0.80 indicated fair agreement, and 0.81 or higher indicated almost perfect agreement.[25]

## Results

Based on the CBCT evaluation, 167 of 367 implants (45.5%) exhibited bone defects at a minimum of 1 site. Table 1 presents the distribution of implants and bone defects detected in each peri-implant region on CBCT images. The values in parentheses represent the numbers of implants with bone defects. The mandibular molar region contained the greatest number of implants (127 of 367, 34.6%), whereas

the mandibular anterior region had the fewest (17 of 367, 4.6%). The highest prevalence rates of bone defects were observed in the maxillary premolar region (27 of 52, 51.9%) and the mandibular molar region (65 of 127, 51.2%).

The CBCT evaluation revealed various patterns of bone defects around the implant fixtures. The findings were as follows: M defects were observed for 3 implants, D for 7, B for 16, L for 2, MD for 8, MB for 1, ML for 1, DB for 4, DL for 2, MDB for 8, MDL for 3, MBL for 1, DBL for 4, and MDBL for 107. The distribution of bone defect patterns was as follows: 28 implants had a defect at 1 site, 32 displayed defects at 2 or 3 sites, and 107 exhibited defects at 4 sites.

The typical sites of bone defects and their detection rates on panoramic images are summarized in Table 2. The most common type of bone defect was circumferential (MDBL; 107 of 167 implants, 64.1%), followed by buccal (B; 16 of 167 implants, 9.6%). Although the number of cases was small, the average detection rate was very low for all defect types other than circumferential. Table 3 presents the number of bone defects for each pattern and the detection rates of defects identified by the 2 observers on panoramic images.

Detection was categorized as either complete, where all bone defect sites around the implant were detectable, or partial, where only some sites were detectable; partial detection represents the detection rate for each M, D, and BL site. For all defect patterns, observer 1, who had more clinical experience, demonstrated a higher detection rate than observer 2. The detection rate tended to increase with the extent of the bone defects (from 1 site to 4 sites). For all bone defect patterns, the rate at which partial defect sites were detected was considerably lower than that for complete defects. Representative panoramic images with high and low detection rates are displayed in Figures 4 and 5. Figure 4 illustrates a case in which a circumferential defect was identified on CBCT, and the observers successfully detected the defect on panoramic imaging. In contrast, Figure 5 depicts a case in which a bone defect on the buccal side was identified on CBCT, but the observers failed to detect this defect on the panoramic image.

Table 4 presents the average AUC values for each region and bone defect site. These values were highest for the anterior region, followed by the premolar and molar regions. Independent of the bone defect site, the lowest AUC value was observed for the anterior teeth of the mandible, while the highest was noted for the maxillary molar region.

Table 5 presents the kappa values for inter-observer agreement in the detection of bone defects on panoramic images. The mandibular premolar region exhibited the highest kappa value. Most regions demonstrated moderate agreement, while the maxillary anterior region displayed the lowest

**Table 1.** Number of implants per region (with bone defects)

|  | Anterior | Premolar | Molar |
|---|---|---|---|
| Maxillary | 43 (15) | 52 (27) | 59 (27) |
| Mandibular | 17 (5) | 69 (28) | 127 (65) |

**Table 2.** Sites of bone defects and their detection rates on panoramic images

| Born defect pattern | 1 site | | | 2 or 3 sites | | | | | | | | | 4 sites |
|---|---|---|---|---|---|---|---|---|---|---|---|---|---|
| Site | M | D | B or L | MD | MB | ML | DB | DL | MDB | MDL | MBL | DBL | MDBL |
| Number | 3 | 7 | 18 | 8 | 1 | 1 | 4 | 2 | 8 | 3 | 1 | 4 | 107 |
| Detection rate (%) | 16.7 | 0 | 0 | 6.3 | 0 | 0 | 0 | 25 | 12.5 | 33.3 | 0 | 0 | 59.8 |

M: mesial, D: distal, B: buccal, L: lingual.

**Table 3.** Detection rates of various bone defect patterns (%)

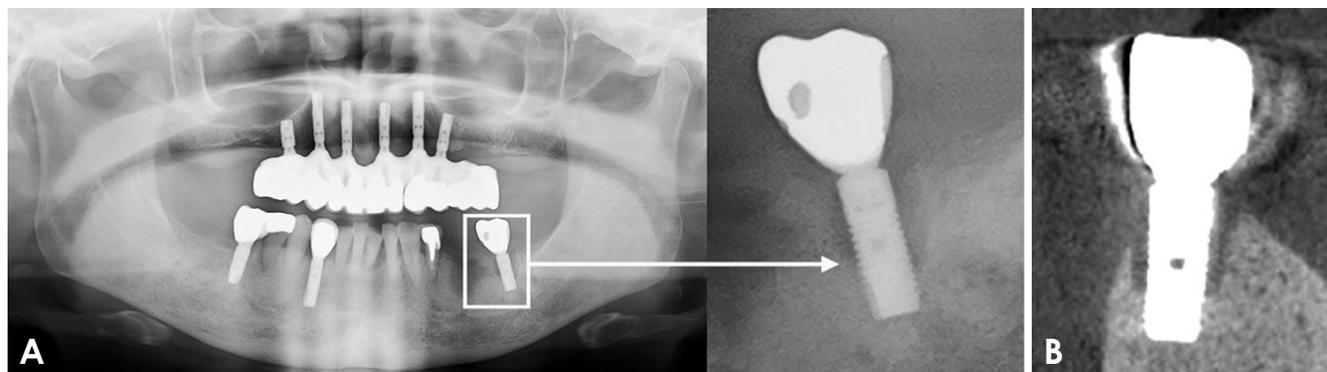| | Observer 1 | | | | Observer 2 | | | |
|---|---|---|---|---|---|---|---|---|
| | Complete detection | Partiaxl detection | | | Complete detection | Partial detection | | |
| | | M | D | B or L | | M | D | B or L |
| 1 site | 3.6 | 0 | 42.9 | 31.6 | 0 | 50.0 | 0 | 15.8 |
| 2 or 3 sites | 18.8 | 50.0 | 52.0 | 47.8 | 0 | 40.0 | 48.0 | 34.8 |
| 4 sites | 72.9 | 53.3 | 56.1 | 55.1 | 46.7 | 34.6 | 37.4 | 31.8 |

**Fig. 4.** A. Panoramic image and enlarged panoramic image. B. Cone-beam computed tomography (CBCT) image (cross-sectional). A circumferential defect was identified on CBCT, and the observers identified the presence of a bone defect on the panoramic image.
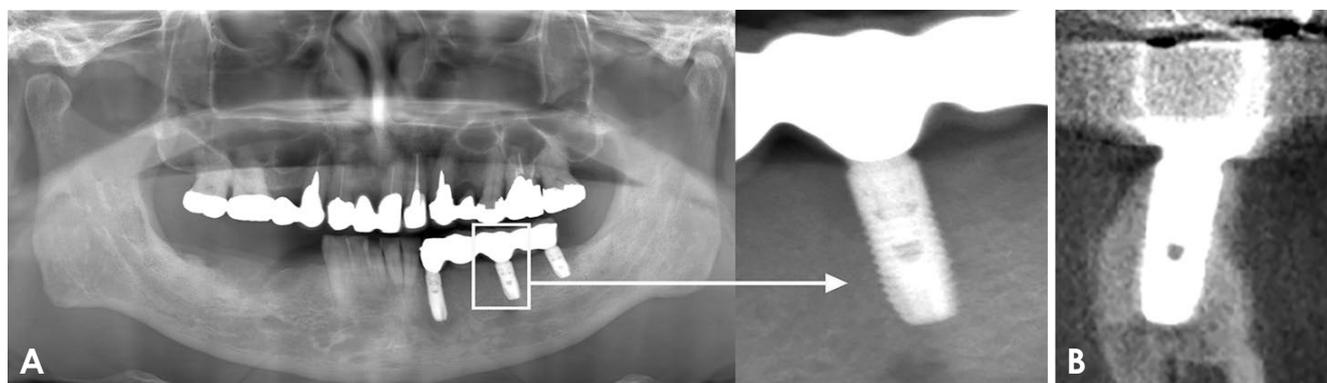


**Fig. 5.** A. Panoramic image and enlarged panoramic image. B. Cone-beam computed tomography (CBCT) image (cross-sectional). The CBCT image revealed a bone defect solely on the buccal side, which the observers were unable to detect on the panoramic image.

**Table 4.** Mean area under the curve across 2 observers by region

| | Maxillary | | | Mandibular | | |
| --- | --- | --- | --- | --- | --- | --- |
| | Anterior | Premolar | Molar | Anterior | Premolar | Molar |
| M | 0.71±0.09 | 0.76±0.01 | 0.82 | 0.57±0.03 | 0.76±0.02 | 0.80±0.03 |
| D | 0.63±0.09 | 0.73±0.01 | 0.82±0.02 | 0.57±0.03 | 0.82±0.04 | 0.83±0.01 |
| BL | 0.55±0.02 | 0.76±0.03 | 0.82±0.08 | 0.48±0.04 | 0.78±0.03 | 0.78 |

M: mesial, D: distal, B: buccal, L: lingual.

**Table 5.** Kappa values for inter-observer agreement in detecting bone defects by region

| | Maxillary | | | Mandibular | | |
| --- | --- | --- | --- | --- | --- | --- |
| | Anterior | Premolar | Molar | Anterior | Premolar | Molar |
| Observer 1 - observer 2 | 0.19 | 0.39 | 0.59 | 0.49 | 0.58 | 0.44 |

kappa value, reflecting poor agreement.

Table 6 presents the kappa values in relation to bone defect type. Although the pattern with 4 sites of bone defect demonstrated a tendency toward higher agreement, the overall rate remained low.

**Table 6.** Kappa values for inter-observer agreement in detecting bone defects by type

|  | 1 site | | | 2 or 3 sites | | | 4 sites | | |
| --- | --- | --- | --- | --- | --- | --- | --- | --- | --- |
|  | M | D | BL | M | D | BL | M | D | BL |
| Observer 1 - observer 2 | 0.28 | 0.19 | 0.14 | 0.05 | 0.10 | 0.19 | 0.24 | 0.20 | 0.20 |

M: mesial, D: distal, B: buccal, L: lingual.

## Discussion

Bone defects were observed for 45.5% of implants, with the most common pattern being the circumferential defect (MDBL; 107/167, 64.1%) (Table 2). Schwarz et al.[13] reported that circumferential defects are the most prevalent type in both humans (55.3%) and dogs (86.6%) with peri-implantitis. García-García et al.[26] similarly found that approximately 30% of defects are circumferential, while another 25% are a combination of circumferential and buccal vertical defects, highlighting the high frequency of circumferential bone defects. Moreover, they noted that peri-implantitis tends to progress circumferentially around the implant.[26] The present study revealed a slightly higher prevalence of circumferential defects compared to previous reports. This discrepancy may stem from the fact that bone defects in earlier studies were observed via flap surgery,[13,26] whereas the current study exclusively utilized CBCT to identify the presence and pattern of bone defects. CBCT images are often compromised by metal artifacts, which can obscure the bone surrounding the implant and potentially "mask" defects.[16,17] Consequently, the detection of small bone defects and the interface between the implant fixture and alveolar bone may not reflect the actual condition.[27] Research also indicates that CBCT imaging accurately captures the morphology of marginal and intraosseous bone defects, while early-stage intraosseous defects are challenging to detect.[28] In the present study, apart from the circumferential defects, partial bone defects included defects on 1 buccal surface (9.6%), defects on 2 M and D surfaces (4.8%), and MD and B defects (4.8%). Similarly, Schwarz et al.[13] described "buccal dehiscence-type defects revealing a semicircular defect" that extend to the center of the implant fixture (15.8%), with cases both involving (13.3%) and not involving (10.2%) the lingual cortex. Although bone resorption typically occurs buccally in the jawbone following tooth loss,[29] it is often necessary to place implants on the buccal aspect to achieve an optimal occlusal relationship, even when buccal bone volume is limited due to post-extraction resorption. In such scenarios, implants are positioned close to the buccal cortical bone, which may lead to thinning of the residual buccal

bone and a heightened risk of bone loss. These factors should be considered when evaluating the presence of bone defects during follow-up.

Bone defects were found to be relatively prevalent in the maxillary premolar and mandibular molar regions. The high frequency of bone defects in the mandibular molar region can be attributed to the greater incidence of tooth loss in this area, which causes more implants to be placed there.[30] As a result, the present study included a comparatively large number of cases and exhibited a high prevalence of bone defects.

The detection rate on panoramic images was highest for circumferential defects (MDBL), at 59.8%. This indicates that panoramic images are valuable as a screening tool for identifying bone defects of this nature. In contrast, the detection rate for partial bone defect sites was low, and defects including DB, M+B or L, and BL+M or D were not detected at all. These findings highlight the challenge of accurately identifying buccolingual bone defects on panoramic images, regardless of the clinician's experience with implant treatment. Since 2-dimensional imaging modalities like panoramic and intraoral radiography cannot distinguish buccolingual bone defects,[28,31] it is difficult to evaluate relatively common partial buccal bone defects, contributing to the risk of misdiagnosis.

The detection rates of bone defects on panoramic images – when categorized by bone defect patterns – appeared to increase with the extent of the defect, from 1 to 4 affected sites (Table 3). This trend was observed regardless of the clinician's years of experience. It was challenging to identify all bone defect sites, even when some were partially detectable. In a previous experiment, Sirin et al.[32] inserted implant fixtures into holes created using 4 types of large drills, with diameters 0.5, 1, 1.5, and 2 mm greater than that of the implant fixture. They then assessed the detection rates of bone defects of varying sizes using 5 different imaging modalities: 2 types of intraoral radiography, panoramic radiography, CBCT, and multidetector computed tomography (MDCT). The authors concluded that panoramic radiography and MDCT are highly reliable for identifying bone defects when the defect's diameter is at least 1.5 mm larger than that of

the implant fixture. In addition, most bone defects identified in the present study were circumferential and larger than the diameter of the implant, which likely contributed to the high detection rate. However, the detection rate for partial defects was low. Defects that did not exceed the diameter of the implant fixture were observed only at the buccal site. This suggests that smaller defects were not identified due to superposition and image distortion,[33] which are common limitations of panoramic radiography. Determining the precise bone morphology from panoramic images is challenging, and patients with clinical findings such as inflammation may have bone defects that cannot be confirmed with conventional 2-dimensional imaging.

To assess the accuracy of evaluations on panoramic images, receiver operating characteristic analysis was conducted using data from the 2 observers, and AUC values were calculated (Table 4). Sirin et al.[32] reported that the AUC for the detection of bone defects with panoramic radiography ranged from 0.72 to 0.82. These figures are comparable to the AUC values for premolars and molars (0.73 to 0.83) observed in the present study. The notable discrepancy in results for the anterior region (particularly in the mandible) between studies results from the fact that in the study by Sirin et al.,[32] the implant bodies were inserted into bovine bone blocks positioned identically to ensure consistent imaging conditions. In contrast, the present study utilized patient images, resulting in variable positioning of the implant fixture relative to the panoramic radiography machine's focal trough and differing inclinations in relation to the X-ray beam, especially in the anterior region. Furthermore, images of the anterior teeth are affected by the ghost image produced by the cervical spine. Additionally, the focal trough of the device is narrower than the width of the molars, leading to the implant fixture often falling partially outside the focal trough due to its greater inclination in the anterior region.[24,34]

The X-ray beam was directed at a more perpendicular angle to the implant fixture in the molar region compared to the anterior region. This orientation facilitated the identification of the thread structures of the implant fixture and enhanced the detection rate of bone defects in the molar region. In the premolar area, however, the AUC values were inconsistent. This variability may be attributed to the pronounced curvature of the dental arch and the greater inclination of the implant fixture in the premolar compared to the molar region.

Observer 1, who possessed more years of experience, demonstrated a higher detection rate of bone defects compared to Observer 2. As the study required the observers to evaluate various implant types, the discrepancy in detection rates between the observers could be attributed to their differing levels of knowledge and familiarity with the structure of each implant system. Nevertheless, even Observer 1 exhibited an inadequate detection rate for bone defects on 1, 2, or 3 lateral sites of the implant fixture. The inter-observer agreement was generally close to moderate, but poor agreement was observed for the maxillary anterior region. As previously mentioned, the lower detection rate and inter-observer agreement in this region may stem from the challenges of depicting implant fixtures on panoramic radiography images, compounded by the impact of the implant placement angle (Table 5). Although the pattern with 4 sites of bone defects exhibited the highest detection rate, the agreement rate was notably low. This suggests that the agreement was suboptimal regardless of the type of bone defect. Furthermore, the substantially lower number of samples with bone defects on 1 to 3 sides, as opposed to those with full circumferential defects, likely contributed to the lower values (Table 6).

As this study was conducted retrospectively and the bone defects were assessed using CBCT images, discrepancies are possible between the observed and actual states of alveolar bone defects due to imaging artifacts. Current guidelines recommend a simple examination method with a low radiation dose during the maintenance period.[4-6] Consequently, panoramic radiography remains a valuable tool, particularly for patients with multiple implants. However, in this study, the detection rate of partial bone defects on panoramic images was insufficient, and issues with standardization and reproducibility are also substantial drawbacks of this imaging modality. One limitation of this study is that it included only 2 observers. Nevertheless, by selecting observers with different levels of experience, insight was gained into the trend that more experienced observers tend to display a higher detection rate of bone defects. In this respect, detailed future research should be conducted, taking into account the number and characteristics of the observers.

Based on this research, clinicians should consider adopting modified imaging techniques that enhance the detection of bone defects without increasing the radiation exposure. Such low-dose conventional radiography methods include the tube-shift technique, which integrates periapical radiography and tomosynthesis with panoramic radiography.

In conclusion, pattern of peri-implant bone defects was found to be circumferential. In cases of partial bone defects, the most common site was the buccal surface alone. This was followed by defects affecting 2 mesiodistal surfaces, and then by defects involving 3 mesiodistal and buccal sur-

faces.

In the observer performance test assessing bone defect detection on panoramic images, the overall detection rate was generally higher in the molar region than in the anterior region. However, the detection rate for partial bone defects was notably low. The detection rate improved as the extent of the bone defects increased, particularly when the defects extended from affecting a single surface of the implant fixture to involving multiple surfaces. The findings of this study suggest that localized peri-implant bone defects, which may develop during post-implantation follow-up, may be overlooked on 2-dimensional panoramic images. Therefore, during follow-up assessments, diagnoses should not rely solely on imaging, but instead should be corroborated by other examinations.

**Conflicts of Interest:** None

## Acknowledgments

## References

1. Schwarz F, Derks J, Monje A, Wang HL. Peri-implantitis. J Clin Periodontol 2018; 45 Suppl 20: S246-66.
2. Renvert S, Persson GR, Pirih FQ, Camargo PM. Peri-implant health, peri-implant mucositis, and peri-implantitis: case definitions and diagnostic considerations. J Periodontol 2018; 89 Suppl 1: S304-12.
3. Heitz-Mayfield LJA, Salvi GE. Peri-implant mucositis. J Clin Periodontol 2018; 45 Suppl 20: S237-45.
4. Harris D, Buser D, Dula K, Grondahl K, Haris D, Jacobs R, et al. E.A.O. guidelines for the use of diagnostic imaging in implant dentistry a consensus workshop organized by the European Association for Osseointegration in Trinity College Dublin. Clin Oral Implants Res 2002; 13: 566-70.
5. Tyndall DA, Price JB, Tetradis S, Ganz SD, Hildebolt C, Scarfe WC, et al. Position statement of the American Academy of Oral and Maxillofacial Radiology on selection criteria for the use of radiology in dental implantology with emphasis on cone beam computed tomography. Oral Surg Oral Med Oral Pathol Oral Radiol 2012; 113: 817-26.
6. Zitzmann NU, Berglundh T. Definition and prevalence of peri-implant diseases. J Clin Periodontol 2008; 35 Suppl 8: 286-91.
7. Patel S, Dawood A, Whaites E, Pitt Ford T. New dimensions in endodontic imaging: part 1. Conventional and alternative radiographic systems. Int Endod J 2009; 42: 447-62.
8. Binon PP. Implants and components: entering the new millennium. Int J Oral Maxillofac Implants 2000; 15: 76-94.
9. Zechner W, Watzak G, Gahleitner A, Busenlechner D, Tepper G, Watzek G. Rotational panoramic versus intraoral rectangular radiographs for evaluation of peri-implant bone loss in the anterior atrophic mandible. Int J Oral Maxillofac Implants 2003; 18: 873-8.
10. Serino G, Turri A. Outcome of surgical treatment of peri-implantitis: results from a 2-year prospective clinical study in humans. Clin Oral Implants Res 2011; 22: 1214-20.
11. Schwarz F, Sahm N, Schwarz K, Becker J. Impact of defect configuration on the clinical outcome following surgical regenerative therapy of peri-implantitis. J Clin Periodontol 2010; 37: 449-55.
12. Wehner C, Bertl K, Durstberger G, Arnhart C, Rausch-Fan X, Stavropoulos A. Characteristics and frequency distribution of bone defect configurations in peri-implantitis lesions - a series of 193 cases. Clin Implant Dent Relat Res 2021; 23: 178-88.
13. Schwarz F, Herten M, Sager M, Bieling K, Sculean A, Becker J. Comparison of naturally occurring and ligature-induced peri-implantitis bone defects in humans and dogs. Clin Oral Implants Res 2007; 18: 161-70.
14. Monje A, Pons R, Insua A, Nart J, Wang HL, Schwarz F. Morphology and severity of peri-implantitis bone defects. Clin Implant Dent Relat Res 2019; 21: 635-43.
15. Pelekos G, Tse JMN, Ho D, Tonetti MS. Defect morphology, bone thickness, exposure settings and examiner experience affect the diagnostic accuracy of standardized digital periapical radiographic images but not of cone beam computed tomography in the detection of peri-implant osseous defects: an in vitro study. J Clin Periodontol 2019; 46: 1294-302.
16. Schulze RK, Berndt D, d'Hoedt B. On cone-beam computed tomography artifacts induced by titanium implants. Clin Oral Implants Res 2010; 21: 100-7.
17. Ritter L, Elger MC, Rothamel D, Fienitz T, Zinser M, Schwarz F, et al. Accuracy of peri-implant bone evaluation using cone beam CT, digital intra-oral radiographs and histology. Dentomaxillofac Radiol 2014; 43: 20130088.
18. Bornstein MM, Horner K, Jacobs R. Use of cone beam computed tomography in implant dentistry: current concepts, indications and limitations for clinical practice and research. Periodontol 2000 2017; 73: 51-72.
19. Harris D, Horner K, Gröndahl K, Jacobs R, Helmrot E, Benic GI, et al. E.A.O. guidelines for the use of diagnostic imaging in implant dentistry 2011. A consensus workshop organized by the European Association for Osseointegration at the Medical University of Warsaw. Clin Oral Implants Res 2012; 23: 1243-53.
20. Kim MJ, Lee SS, Choi M, Yong HS, Lee C, Kim JE, et al. Developing evidence-based clinical imaging guidelines of justification for radiographic examination after dental implant installation. BMC Med Imaging 2020; 20: 102.
21. Heuberer S, Dvorak G, Mayer C, Watzek G, Zechner W. Dental implants are a viable alternative for compensating ologodontia in adolescents. Clin Oral Implants Res 2015; 26: e22-7.

22. Geraets WG, Verheij HG, Wismeijer D, van der Stelt PF. Detecting bone loss along dental implants by subtraction of panoramic radiographs. Clin Oral Implants Res 2012; 23: 861-5.

23. Merheb J, Graham J, Coucke W, Roberts M, Quirynen M, Jacobs R, et al. Prediction of implant loss and marginal bone loss by analysis of dental panoramic radiographs. Int J Oral Maxillofac Implants 2015; 30: 372-7.

24. Suomalainen A, Pakbaznejad Esmaeili E, Robinson S. Dento-maxillofacial imaging with panoramic views and cone beam CT. Insights Imaging 2015; 6: 1-16.

25. Landis JR, Koch GG. The measurement of observer agreement for categorical data. Biometrics 1977; 33: 159-74.

26. García-García M, Mir-Mari J, Benic GI, Figueiredo R, Valmaseda-Castellón E. Accuracy of periapical radiography in assessing bone level in implants affected by peri-implantitis: a cross-sectional study. J Clin Periodontol 2016; 43: 85-91.

27. Benic GI, Sancho-Puchades M, Jung RE, Deyhle H, Hämmerle CH. In vitro assessment of artifacts induced by titanium dental implants in cone beam computed tomography. Clin Oral Implants Res 2013; 24: 378-83.

28. Golubovic V, Mihatovic I, Becker J, Schwarz F. Accuracy of cone-beam computed tomography to assess the configuration and extent of ligature-induced peri-implantitis defects. A pilot study. Oral Maxillofac Surg 2012; 16: 349-54.

29. Pietrokovski J, Massler M. Alveolar ridge resorption following tooth extraction. J Prosthet Dent 1967; 17: 21-7.

30. Jang HW, Kang JK, Lee K, Lee YS, Park PK. A retrospective study on related factors affecting the survival rate of dental implants. J Adv Prosthodont 2011; 3: 204-15.

31. Rees TD, Biggs NL, Collings CK. Radiographic interpretation of periodontal osseous lesions. Oral Surg Oral Med Oral Pathol 1971; 32: 141-53.

32. Sirin Y, Horasan S, Yaman D, Basegmez C, Tanyel C, Aral A, et al. Detection of crestal radiolucencies around dental implants: an in vitro experimental study. J Oral Maxillofac Surg 2012; 70: 1540-50.

33. Lam EW, Ruprecht A, Yang J. Comparison of two-dimensional orthoradially reformatted computed tomography and panoramic radiography for dental implant treatment planning. J Prosthet Dent 1995; 74: 42-6.

34. Riecke B, Friedrich RE, Schulze D, Loos C, Blessmann M, Heiland M, et al. Impact of malpositioning on panoramic radiography in implant dentistry. Clin Oral Investig 2015; 19: 781-90.